Visual Neuroscience (2002), **19**, 109–118. Printed in the USA.

DOI: 10.1017.S0952523802191103

Differential distributions of red–green and blue–yellow cone opponency across the visual field

KATHY T. MULLEN AND FREDERICK A.A. KINGDOM

McGill Vision Research, Department of Ophthalmology, McGill University, 687 Pine Avenue West (H4-14), Montreal, Canada H3A 1A1

(RECEIVED August 23, 2001; ACCEPTED January 13, 2002)

Abstract

The color vision of Old World primates and humans uses two cone-opponent systems; one differences the outputs of L and M cones forming a red–green (RG) system, and the other differences S cones with a combination of L and M cones forming a blue–yellow (BY) system. In this paper, we show that in human vision these two systems have a differential distribution across the visual field. Cone contrast sensitivities for sine-wave grating stimuli (smoothly enveloped in space and time) were measured for the two color systems (RG & BY) and the achromatic (Ach) system at a range of eccentricities in the nasal field (0–25 deg). We spatially scaled our stimuli independently for each system (RG, BY, & Ach) in order to activate that system optimally at each eccentricity. This controlled for any differential variations in spatial scale with eccentricity and provided a comparison between the three systems under equivalent conditions. We find that while red–green cone opponency has a steep decline away from the fovea, the loss in blue–yellow cone opponency is more gradual, showing a similar loss to that found for achromatic vision. Thus only red–green opponency, and not blue–yellow opponency, can be considered a foveal specialization of primate vision with an overrepresentation at the fovea. In addition, statistical calculations of the level of chance cone opponency in the two systems indicate that selective S cone connections to postreceptoral neurons are essential to maintain peripheral blue–yellow sensitivity in human vision. In the red–green system, an assumption of cone selectivity is not required to account for losses in peripheral sensitivity. Overall, these results provide behavioral evidence for functionally distinct neuro-architectural origins of the two color systems in human vision, supporting recent physiological results in primates.

Keywords: Color vision, Cones, Cone opponency, Periphery, Isoluminance, Blue–yellow

Introduction

It is well accepted that the early stages of primate color vision are mediated by two cone-opponent processes, loosely termed "red–green" and "blue–yellow." The red–green opponent system differences the L and M cone outputs, whereas the blue–yellow pits the S cones against a combination of L and M cones. Initially, it was believed that all primate color vision, including both the red–green and blue–yellow cone-opponent systems, was mediated by the parvocellular subcortical pathway (e.g. Derrington et al., 1984; Valberg et al., 1986; Shapley & Perry, 1986; Lee et al., 1987). Results emerging over the last decade, however, have altered this view. Intracellular retinal recordings and neuroanatomy suggest that the red–green and blue–yellow cone-opponent classes have distinct cell morphologies, physiologies, and may occupy distinct retino-cortical streams. In the retina, the blue–yellow system is now thought to have its own specialized midget bipolar cells and small-field bistratified ganglion cells (Mariani, 1984; Gouras, 1991; Rodieck & Watanabe, 1993; Dacey, 1993*a*; Dacey & Lee, 1994; Dacey, 1996; Calkins et al., 1998). At the level of the lateral geniculate nucleus (LGN), results also suggests that S cone-opponent neurons occupy a separate pathway, as S cone opponency has been reported in the koniocellular LGN layers of both New World (Martin et al., 1997) and Old World monkeys (Hendry & Reid, 2000). Thus the koniocellular pathway may represent a functional LGN stream for S cone opponency, although further data are required to establish this definitively (Goodchild & Martin, 1998). At the cortical level of V1, there is also evidence suggesting that red–green and blue–yellow cone-opponent pathways remain segregated (Ts'o & Gilbert, 1988), although this remains controversial (Lennie et al., 1990).

The distinctive cytoarchitecture of the red–green and blue–yellow cone-opponent pathways is matched by a distinctive evolutionary history, with molecular genetic evidence to suggest quite different evolutionary time scales. Trichromacy, which supports the L,M (red–green) cone-opponent pathway, is believed to have evolved relatively recently in mammals, and with rare exceptions

Address correspondence and reprint requests to: Kathy T. Mullen, McGill Vision Research, Department of Ophthalmology, McGill University, 687 Pine Avenue West (H4-14), Montreal, Canada H3A 1A1. E-mail: kathy.mullen@mcgill.ca

is exclusive to Old World primates (Nathans et al., 1986; Mollon, 1989, 1993; Nathans, 1999). On the other hand, the ancestral cone pigments of dichromatic mammals, which support only blue–yellow cone opponency, are believed to have existed since the emergence of a second opsin gene about 500 million years ago (Nathans, 1987).

These cyto-architectural differences between the red–green and blue–yellow cone-opponent systems, which have only recently emerged in the literature, are likely to have behavioral consequences for human vision. In this paper, we address the issue of the loss of color sensitivity across the visual field. Our aim is to compare the distributions across the visual field of the red–green and blue–yellow cone-opponent mechanisms in human vision, as distinct postreceptoral distributions would be supporting behavioral evidence for functionally distinct neuro-architectural origins for the two systems. It has already been established that our fovea has a strong specialization for red–green color vision, demonstrated by the very steep declines in red–green visual acuity and contrast sensitivity across the visual field relative to achromatic (luminance) sensitivity (Mullen, 1991; Anderson et al., 1991; Mullen & Kingdom, 1996). As most visual functions decline across the visual field, it is the fact that these losses of acuity and contrast sensitivity are much greater than the equivalent ones found for achromatic vision that demonstrates a specific clustering of the red–green mechanisms of human color vision to central vision. Furthermore, the origin of this specialization is postreceptoral, since both achromatic and red–green systems originate from common L and M cone types. The origin of the foveal strength of red-green color vision is presently controversial, but is thought to be linked to the preponderance of midget bipolar and ganglion cells in the primate retina, which are found predominantly in the central visual field (Shapley & Perry, 1986; Dacey, 1993*b*; Wassle et al., 1994; Boycott & Wassle, 1999). As evidence is now emerging that blue–yellow cone opponency is not mediated by these retinal P cells, but by a different subcortical pathway, there is no reason to suppose that the red–green and blue–yellow cone-opponent systems are distributed similarly across the visual field. So far, no studies have addressed this issue systematically (but see Mullen et al., 2000).

In this paper, we compare how the cone contrast sensitivities of the isolated red–green, blue–yellow, and achromatic mechanisms of human vision vary across the visual field under equivalent stimulus conditions.* One of the difficulties in making such a comparison between the three postreceptoral mechanisms (red–green, blue–yellow, and achromatic) is to determine the conditions for the comparison. Equivalent conditions must take into account, for example, the difference in the spatio-temporal contrast sensitivity functions and spatial summation between the three mechanisms, and how these may vary differentially with eccentricity. In this paper, we do not use a common magnification factor to scale our stimuli, since this might not be appropriate for all three postreceptoral mechanisms. Instead we scaled the stimuli individually by selecting the spatio-temporal conditions that provided peak sensitivity for each mechanism at each eccentricity. Our results show that only red–green cone opponency can be considered a foveal specialization, since blue–yellow cone opponency is more uniformly distributed across the visual field, and more closely resembles the distribution of the achromatic system. Additionally, in this paper we point out differential statistical limitations on cone opponency in the two systems arising from the sparser distribution of S cones in the population compared to the L and M. We show that, statistically, as the numbers of cones in a receptive field increases, cone opponency arising from unselective (hit & miss) cone projections can be better sustained in an L,M cone-opponent system than in an S cone one. This limitation, inherent in the photoreceptor distribution, highlights cone-selective projections as the essential underpining of blue–yellow cone opponency in human vision.

*When measured psychophysically, the cone-opponent systems are commonly termed "mechanisms."

Methods

Stimuli

Stimuli were tall strips of horizontal sine-wave grating patches, presented in a contrast envelope with the form of a raised cosine with a flat top. The height of the stimulus strip (i.e. along the modulated axis of the grating) was given by the number of sine-wave grating cycles displayed in the flat top of the contrast envelope, and was 3 or 4 cycles. Both the height (in grating cycles) and the spatial frequency of the grating were selected to optimize cone contrast sensitivity as part of the experiments described below. Gratings were sharply truncated in the nonmodulated (horizontal) dimension at a full width of 2 grating cycles. A smaller width than height was chosen in order to confine the grating in eccentricity without compromising spatial summation in cycles along the modulated grating axis. The viewing distance was 155 cm, but reduced to 78 cm for the lowest spatial frequencies used [0.3 cycles/deg (cpd)]. Gratings were static and presented in a temporal contrast window with the form of a Gaussian envelope (σ = 125 ms). Stimuli were displayed on the horizontal meridian of the nasal visual field between 0 and 25 deg.

Three types of test stimuli were used, corresponding to the cardinal stimuli for each of the three postreceptoral detection mechanisms or systems (red–green, blue–yellow, and luminance). Stimuli were defined within a cone-contrast space that directly represents the outputs of the three cone responses. This stimulus space, denoted by (L, M, & S), is defined as the incremental quantal catches of the three cone types to a given stimulus, normalized by the respective quantal catches to the fixed white background. The three stimuli, described within this cone-contrast space, were each selected to activate a single postreceptoral mechanism in isolation, and so are termed cardinal (Krauskopf et al., 1982; Derrington et al., 1984; Cole et al., 1993; Sankeralli & Mullen, 1997). From previous determinations of the mechanism directions in this space, we selected an achromatic and a blue–yellow cardinal axis that modulate the (L, M, & S) cone responses in the ratios of 1:1:1 (achromatic) and 0:0:1 (blue/yellow), respectively (Sankeralli & Mullen, 1996, 1997). Note these also correspond to the cardinal axes used in a cone-excitation space used by Krauskopf et al. (1982) and Derrington et al. (1984). Contrast is defined as the vector length (stimulus contrast) for each of the three cardinal stimuli in cone contrast units.

For the red–green cardinal axis, an individual determination of isoluminance was obtained for each subject at each eccentric location tested, using a minimum motion paradigm (Mullen & Sankeralli, 1999). This was done in order to take into account the intersubject variability in the L and M cone weights to the luminance mechanism (Stromeyer et al., 1997) and the potential variation in isoluminance across the visual field. In addition, if high contrast eccentrically viewed chromatic stimuli became achro-

matic in appearance, data were not collected for that condition. Owing to the large size of the test stimuli, accurate corrections for the variations in macular pigment across the visual field could not be made. Instead, the accuracy of S cone isolation was checked using a minimum sensitivity paradigm, in which the chromatic vector direction of a grating test stimulus is varied systematically within the plane formed by the red–green cardinal axis and the blue–yellow cardinal axis (S cone). The subject determines, using a method of adjustment, the vector direction in which the stimulus (of fixed contrast) is least visible. The vector direction with the poorest visibility indicates the direction of S cone isolation (e.g. Sankeralli & Mullen, 1996). In all cases these directions closely conformed to the calibrated S cone axis, confirming its accuracy. We also note that the lowpass low-resolution shapes of the cone contrast sensitivity functions obtained in the study support the accurate determination of isoluminance.

The stimulus was presented on a BARCO CCID 7651 RGB monitor, with a frame rate of 75 Hz and a line rate of 60 kHz, driven by a video controller (Research Systems VSG2/1) interfaced with a Dell 333D computer. The video light output was linearized in VSG software to within a contrast error of 0.17 log units. The screen (13 deg $\times$ 10 deg at 155 cm) was fixed at a background luminance of 55 cd m^{-2} near equal energy white [CIE (0.28, 0.30)].

Procedure and subjects

Contrast thresholds were measured using a standard two AFC staircase procedure. Each trial consisted of two intervals, one containing the test and the other containing a blank. The subject was required to identify which presentation contained the test. Each interval was preceded by a brief tone, and a small spot was continuously placed at the fixation point. Audio feedback informed the subject whether their response was correct or not. In the staircase procedure the test contrast was raised by 0.10 units following an incorrect response, and lowered by 0.05 units following two consecutive correct responses. The threshold value was evaluated as the mean of the last six reversals of the staircase. This value estimated the 81.6% correct level for this task. Each threshold data point was obtained as the average of at least three measurements. Two color-normal subjects (the authors) performed the experiments.

Results

A comparison of blue–yellow, red–green, and achromatic cone contrast sensitivity across the visual field

We aim to compare the changes in cone contrast sensitivity across the visual field for the red–green, blue–yellow, and achromatic postreceptoral mechanisms. Before this can be done, a number of control experiments are required to ensure that any apparent loss in contrast sensitivity with eccentricity is not a consequence of the particular choice of stimulus parameters. In the first control experiment, we establish the test spatial frequency to be used at each eccentricity for each mechanism. If a single fixed spatial frequency was used to test all mechanisms at all retinal locations, differential changes in the shapes of the contrast sensitivity functions (CSF) of the three mechanisms with eccentricity could produce apparent losses in contrast sensitivity that would depend on the spatial frequency used. Furthermore, as maximum contrast sensitivity shifts to lower spatial frequencies with eccentricity, a stimulus of fixed spatial frequency would be testing different relative parts of the CSF at different retinal locations. To avoid these problems, we selected the spatial frequency that produces optimal cone contrast sensitivity for each system at each retinal location, thus applying a spatial scaling to each system individually across eccentricity. To obtain these data, we measured complete contrast sensitivity functions at every 5 deg of eccentricity, from the fovea to 25 deg for the red–green, blue–yellow, and achromatic mechanisms. Data for sample locations of 0, 10, and 20 deg are shown in Fig. 1. For these functions, 4 spatial cycles were displayed in each stimulus. Results show that both the cone-opponent mechanisms (red–green and blue–yellow) have lowpass contrast sensitivity functions, in comparison to the more bandpass function of achromatic vision, as expected from previous literature (Granger & Heurtley, 1973; Kelly, 1983; Mullen, 1985; Humanski & Wilson, 1992). All functions show an increasing loss in cone contrast sensitivity to the higher spatial frequencies as eccentricity increases, reflecting changes in the spatial scaling of vision with eccentricity. It is also interesting to note from this figure that, at the fovea, the red–green mechanism is the most sensitive in terms of cone contrast units over the spatial-frequency range tested. However, its sensitivity collapses dramatically at 10 and 20 deg in comparison to the blue–yellow and achromatic mechanisms, which show a much smaller loss.

From these data, we selected spatial frequencies that would yield the peak contrast sensitivities at each eccentricity for each mechanism. For the lowpass red–green and blue–yellow mechanisms, in which maximum contrast sensitivity occurs at low spatial frequencies, we selected a test stimulus of 0.3 cpd at all eccentricities. For the achromatic mechanism, the contrast sensitivity data were fitted with a polynomial function, and the spatial frequency at which a peak in cone contrast sensitivity occurs was obtained from the fit. Lower spatial frequencies were selected at greater eccentricities, ranging from 1 cpd at the fovea to 0.3 cpd (for KTM) or 0.4 cpd (for FAK) at 25 deg of eccentricity.

The choice of stimulus size is also restricted. Stimuli must be confined in space to allow different retinal locations to be tested separately, but also must contain sufficient spatial cycles to be detectable in the periphery with no loss of relative sensitivity between the three mechanisms arising from any differential requirements in spatial summation. In a second control experiment, we measured the effects of summation in grating cycles at two different eccentricities for the three visual mechanisms (RG, BY, & Ach). The number of grating cycles in the flat top of the cosine envelope was varied from 3 to 8 at the fovea and at 20 deg, using the preferred spatial frequency of each mechanism for the eccentricity tested. We found no significant increase in cone contrast sensitivity between 3 and 8 spatial cycles for either the chromatic or the luminance mechanisms. We therefore selected a stimulus with 3 spatial cycles as the smallest available that produces asymptotic, or near asymptotic, spatial summation for all three mechanisms. (Note that this replaces the stimulus size of 4 spatial cycles used in Fig. 1).

Measurements of cone contrast sensitivity were obtained using the preferred spatial frequency and stimulus size for each visual mechanism, sampling across the nasal visual in steps of 5 deg. Fig. 2 shows the results. Cone contrast sensitivity is very high for the red–green cone-opponent system in the fovea, but declines steeply across the visual field. The blue–yellow system, on the other hand, shows a much shallower decline in cone contrast sensitivity across the visual field, displaying a similar pattern of

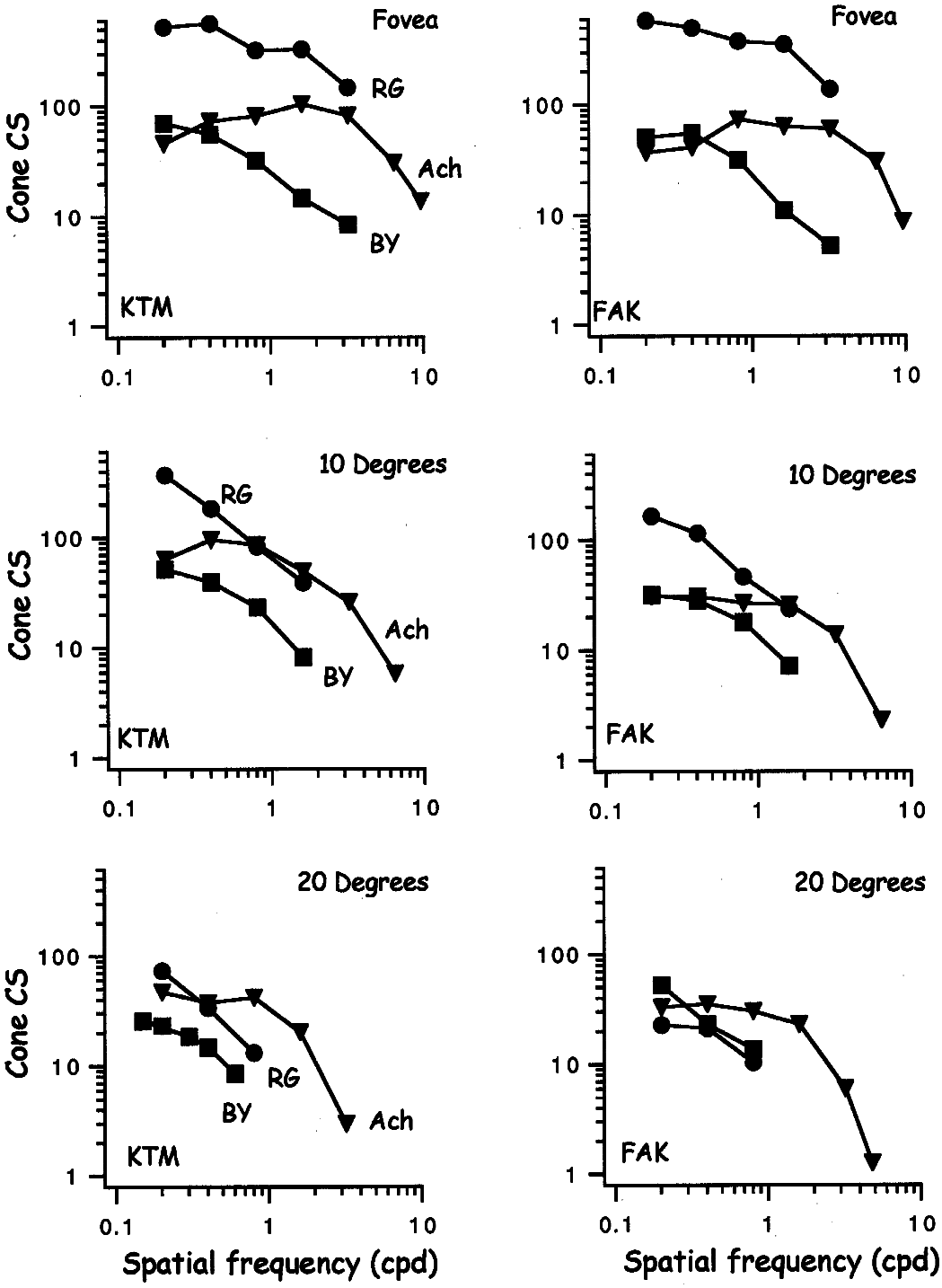

Fig. 1. Cone contrast sensitivity functions are shown for stimuli that isolate the red–green (circles) and blue–yellow (squares) cone-opponent mechanisms, and the achromatic mechanism (triangles). Stimuli extend for 4 spatial cycles in the modulated (vertical) direction and 2 cycles in the unmodulated (horizontal) direction. Sample data are shown for 0, 10, and 20 deg of eccentricity, but functions were obtained in 5-deg steps from 0 deg to 25 deg. Each achromatic function was fitted with a third-order polynomial to determine the spatial frequency at peak cone contrast sensitivity.

loss to the achromatic mechanism. Thus, the red–green and blue–yellow mechanisms display fundamental differences in the form of their loss in cone contrast sensitivity across eccentricity.

Most visual functions decline with eccentricity, and so whether a visual loss across eccentricity is steep or not depends on with what it is compared. In Fig. 3, we compare the loss of blue–yellow (left) and red–green (right) cone contrast sensitivity with the loss of achromatic sensitivity. The ratio of the two sensitivities (color/achromatic) normalized at the fovea is plotted as a function of eccentricity. This comparison shows that red–green cone oppo-

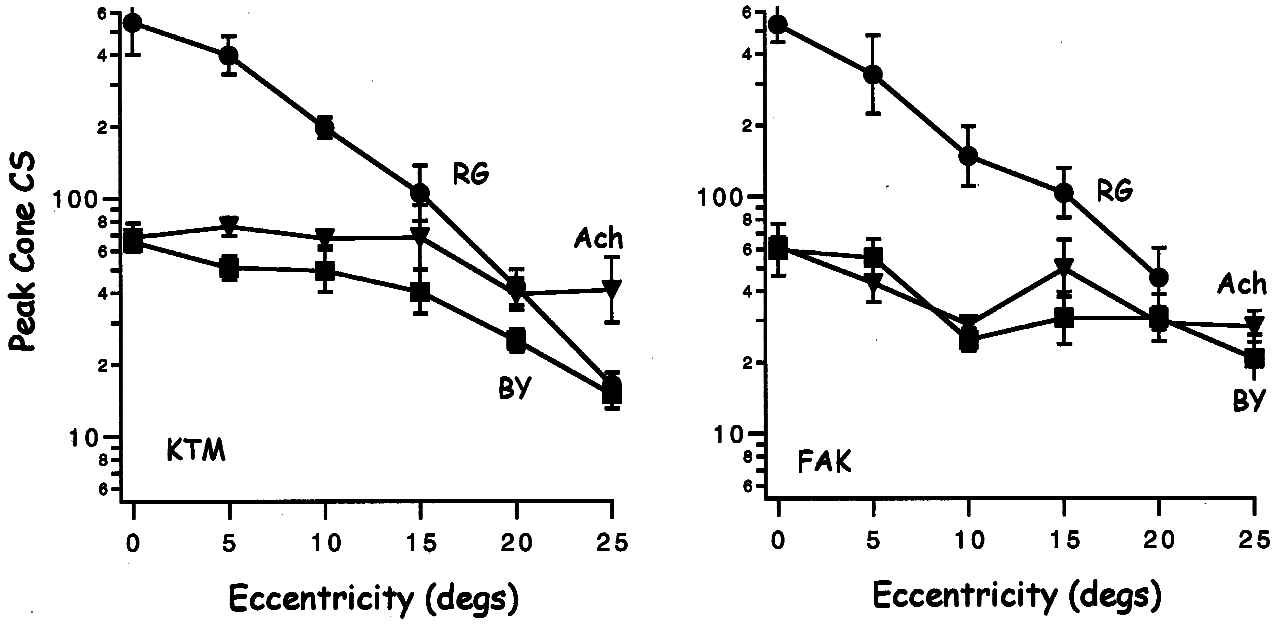

Fig. 2. Peak cone contrast sensitivity is shown for stimuli that isolate the red–green (circles) and blue–yellow (squares) cone-opponent mechanisms, and the achromatic mechanism (triangles) as a function of eccentricity in the nasal field. Stimulus size is 3 spatial cycles in the modulated (vertical) direction and 2 cycles in the unmodulated (horizontal) direction. The stimulus spatial frequency was determined from the maxima of the cone contrast sensitivity functions of Fig. 1. For the chromatic stimuli, the spatial frequency was 0.3 cpd, and for the achromatic stimuli the spatial frequency depended on eccentricity. (For FAK: $sf = 1.0, 0.61, 0.55, 0.41, 0.41,$ & 0.41 cpd; and for KTM: $sf = 1, 0.63, 0.52, 0.35, 0.3,$ & 0.3 cpd at eccentricities of 0, 5, 10, 15, 20, & 25 deg, respectively). No red–green threshold could be obtained for FAK at 25 deg. Error bars show ± 1 SD.

nency declines steeply away from the fovea with a much greater loss than achromatic sensitivity, whereas blue–yellow cone opponency is much better maintained, following a pattern more similar to achromatic sensitivity over the region tested. These differences suggest that the distributions of the red–green and blue–yellow cone-opponent mechanisms across the visual field are very different. The dashed line in Fig. 3 is the statistical prediction of the loss in cone opponency based on unselective cone projections, explained next.

Chance cone opponency in the blue–yellow and red–green systems

We have previously pointed out how unselective ("hit and miss") postreceptoral projections of the L and M cones to the postreceptoral neurons would predict a loss of red–green cone opponency with increasing receptive-field size across the visual field (Mullen & Kingdom, 1996). Later, in the Discussion, we critically examine this model of red–green cone-opponency in the light of recent neurophysiological findings. Here we consider whether, in principle, such a model is applicable to the blue–yellow cone-opponent system in the light of the results of this study. This forms the basis for a statistical argument for why cone-selective connections are essential for blue–yellow cone opponency in human vision. Cone opponency depends on a difference in spectral sensitivity between the excitatory and inhibitory signals to a particular neural unit. Any neuron with a differential proportion of cone types feeding the inhibitory and excitatory regions of its receptive field is cone opponent and thus color sensitive. Some cone opponency will arise if cones project unselectively to postreceptoral neurons because, by chance, differential proportions of the cone types are bound to fall within the excitatory and inhibitory regions of a receptive field. As the population of cones sampled by a receptive field increases in size, the effects of these chance (binomial) variations will be reduced, and "hit & miss" cone opponency will be lost. Assuming a random cone mosaic (Mollon & Bowmaker, 1992) and indiscriminate postreceptoral cone projections, one can calculate the theoretical binomial limitation on S cone compared to L,M cone opponency that occurs as the number of cones in a receptive field increases.

In Fig. 4, we plot the binomial calculations of how the chance differential distributions of S cones to the center and surround of a receptive field vary as the size of the cone group increases. This is compared with the same calculations as applied to the L,M cone system. We use as our example a center-surround unit with six times as many cones in the surround than the center, and with equal gains for the center and surround. The measure we calculate is termed "average cone-opponent purity", and is given by summing the binomial probabilities for all possible combinations and permutations of cones in both the center and surround of a unit (see legend). Appendix 1 shows the full calculations for the S cone-opponent system, and calculations for the L,M cone-opponent system have been published previously (Mullen & Kingdom, 1996). Fig. 4 plots the average cone-opponent purity in the two systems as a function of the center size of the receptive field. The calculations show that cone opponency, based on binomial variation in the proportions of cone types in a receptive-field center and surround, declines more steeply for the blue–yellow cone-opponent system than for the red–green.

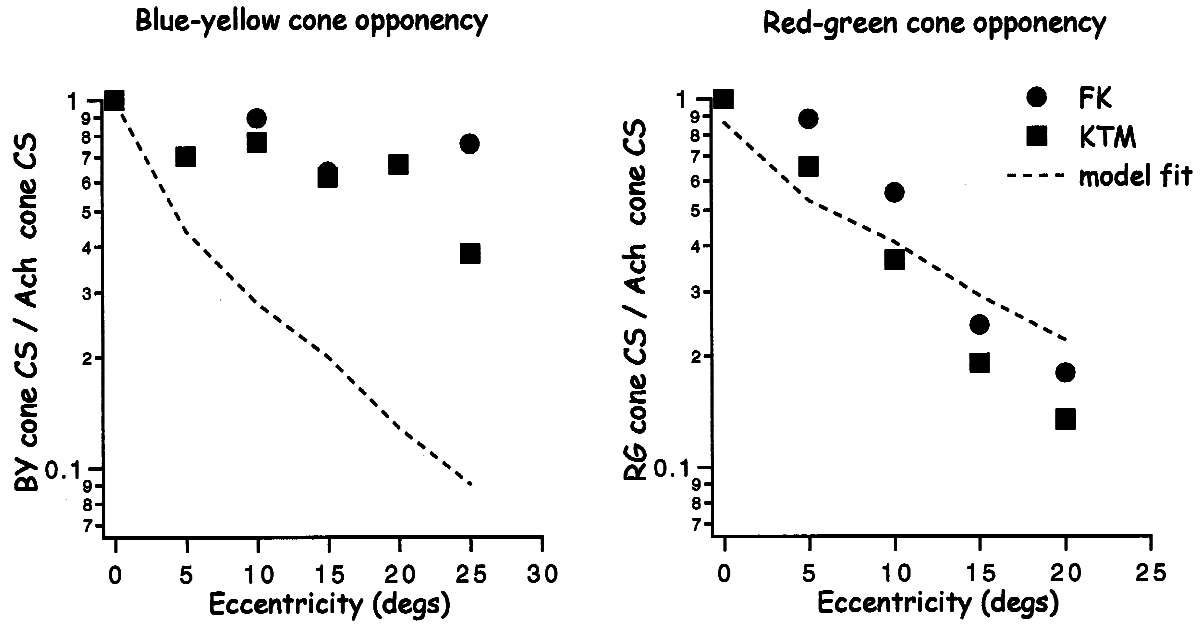

Fig. 3. Data points show the ratio of color to achromatic cone contrast sensitivities for the blue–yellow (left) and red–green (right) cone-opponent systems normalized at the fovea. Data are from Fig. 2. Results are for two subjects. The dashed line is the fit of the binomial model to the data (see text).

The dashed lines in Fig. 3 give the fits of these calculations to the psychophysical data. To turn these binomial calculations into a model of the human psychophysical data, an estimate of the average number of cones supplying receptive fields of the retinal cells at each eccentricity is required. As such data are not directly available, we have estimated the average number of cones per receptive field using cone density data from human retina (Curcio et al., 1991) and the average center size of macaque P retinal ganglion cells as a function of eccentricity (Croner & Kaplan, 1995), following Mullen and Kingdom (1996). The model was fitted to the data by calculating a minimum chi-squared statistic for the combined data of the two subjects.†

This model (dashed lines) shows that the empirical loss in blue–yellow cone opponency differs dramatically from the predictions of unselective cone projections. As previously shown (Mullen & Kingdom, 1996), the steep loss in red–green cone opponency across the visual field does not require the assumption of selectivity, since the loss is similar to that predicted from the binomial variation in unselective cone combinations. On the other hand, human blue–yellow cone contrast sensitivity is well maintained relative to achromatic sensitivity across the visual field, and thus must be supported by selective cone connections in human vision.

†As a measure of the goodness of fit of the model to the red–green cone contrast sensitivity data, we calculated for each subject a minimum chi-squared fit of the model to the data. The chi-squared values obtained were 3.52 (FAK) and 6.47 (KTM). With 4 deg of freedom (five data point minus one free parameter) this yields Q values of 0.474 and 0.166, respectively. Values of $Q > 0.1$ are considered to indicate an acceptable fit of a model to the data. The dashed line is thus an acceptable fit to the data for both subjects. Note the fit only affects the vertical displacement of the model, and so has one free parameter.

Discussion

Past studies have shown that color vision can be supported in the periphery at least up to 80 deg, and that foveal color discrimination is superior (Baird, 1905; Rand, 1913; Gordon & Abramov, 1977; Van Esch et al., 1984). These studies, however, have not separated the performances of the two postreceptoral cone-opponent mechanisms. Our results demonstrate that it is important to do this, since the red–green and blue–yellow cone-opponent mechanisms have very different distributions across the visual field. In previous publications we, and others, have demonstrated that L,M (red–green) cone opponency sharply peaks in the fovea, in both contrast sensitivity (Mullen, 1991; Stromeyer et al., 1992; Mullen & Kingdom, 1996; Pearson & Swanson, 2000) and acuity (Anderson et al., 1991). Fig. 3 of this study specifically compares the loss in red–green contrast sensitivity with that for the achromatic system under equivalent conditions, and shows the red–green contrast sensitivity loss to be much greater; for example at 20 deg, the loss in red–green contrast sensitivity is 85% greater than the loss in achromatic sensitivity. This type of comparison has revealed that red–green color vision is a primate foveal specialization (Mullen, 1991; Mullen & Kingdom, 1996). Moreover, because the L and M cones are common to both the achromatic (luminance) system and the L,M cone-opponent system, this red–green foveal specialization is postreceptoral in origin.

S-cone-based (blue–yellow) color vision, on the other hand, shows a shallower decline in sensitivity across the visual field, resembling the loss in achromatic sensitivity (Fig. 2). In fact, the calculated ratio of blue–yellow to achromatic sensitivity (Fig. 3) shows a function that is relatively flat with eccentricity. Comparing all three mechanisms (red–green, blue–yellow, and achromatic) in terms of their peak contrast sensitivities, we see that at the fovea the red–green cone-opponent mechanism is considerably more sensitive, but by 20 deg all three are quite similar. Thus, any

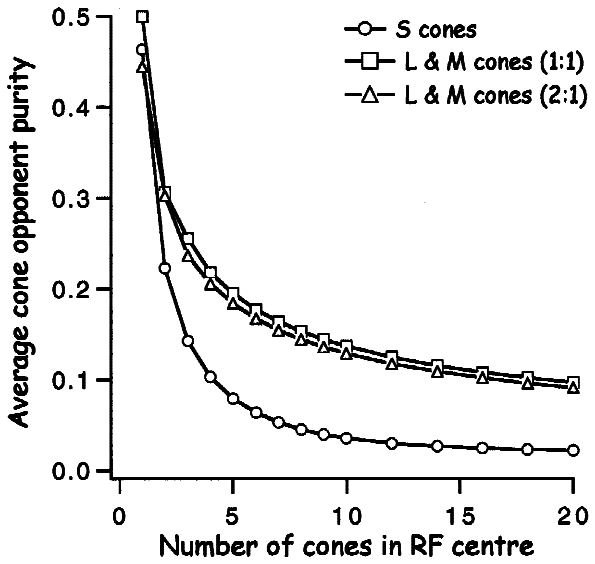

Fig. 4. Average cone opponency arising from binomial variations in the proportions of cone types in the excitatory and inhibitory regions of a receptive field, as a function of the number of cones in the unit. Average cone-opponent purity is a statistical measure of the average differential distribution of cone types to the center and surround of a receptive field of a particular center size, and indicates the degree of cone opponency that arises by chance. Note that even though the maximum possible cone-opponent purity for an individual unit is 1 (e.g. an all S cone center with no S cones in the surround, or a pure L cone center with a pure M cone surround, etc.), the average cone-opponent purity is much less because this calculation takes into account the probabilities of each occurrence. Thus cone-opponent purity applies to a particular unit, whereas *average* cone-opponent purity applies to a population of units all drawing on the same number of cones. Calculations are for L,M cone opponency with equal numbers of L and M cone types ($P = 0.5$) (squares), or L and M cones in the ratio of 2:1 ($P = 0.67$) (triangles); and for S cone opponency with S cones forming 7% of the population ($P = 0.7$) (circles). An S cone-opponent unit is defined as one with a least one S cone in the center. Calculations for S cone opponency are given in Appendix 1, and for L,M opponency are in Mullen and Kingdom (1996).

chromatic stimulus that is not designed to separate between the responses of the two cone-opponent mechanisms is likely to be detected by a composite response whose make-up will shift as the stimulus moves from fovea to periphery. Furthermore, claims that color vision is selectively impaired away from the fovea (Mullen, 1991; Martin et al., 2001) should be specifically confined to the red–green cone-opponent system, since they do not apply to the blue–yellow system.

As pointed out in the Introduction, the means of comparing the contrast sensitivities of the three mechanisms across eccentricity needs careful consideration as it influences the results obtained. Specifically, the stimulus parameters must be varied across the visual field to allow some compensation for the overall physiological changes in the visual system that occur with eccentricity, notably the increase in average receptive-field size and in the decrease in the density of the neural representation. Some studies have size-scaled spot stimuli in an attempt to compensate for changes in cone density, ganglion cells spacing, or cortical magnification (Van Esch et al., 1984), while others have increased the spot size unsystematically in the periphery (Gordon & Abramov, 1977; Stromeyer et al., 1992) or used a fixed spot size (Pearson & Swanson, 2000; Martin et al., 2001). While all methods still reveal a superiority of color vision in the fovea, in this paper we are more interested in the quantitative comparison between the three mechanisms across eccentricity, and in the specific form of the contrast sensitivity loss. For this, we need a strong rationale for the selection of appropriate stimulus parameters. We have scaled our grating stimulus parameters with eccentricity selectively for each mechanism, so as to achieve a peak in cone contrast sensitivity for each mechanism at each eccentricity tested. The aim of this is to ensure that the most sensitive population of neurons is activated for each mechanism at each eccentricity.

Since the two color mechanisms have lowpass contrast sensitivity functions, we were able to use the same low spatial frequency at all eccentricities (0.3 cpd). At the greater eccentricities, additional measurements showed that a lower spatial frequency (0.2 cpd) would have slightly improved red–green cone contrast sensitivity. We did not, however, switch to this spatial frequency because of its impact on stimulus localization; as the stimulus window gets larger to maintain a constant spatial number of spatial cycles, it is less confined in eccentricity. Also, such a change would not have significantly modified our results. We note that for the luminance mechanism, with its bandpass contrast sensitivity function, the spatial frequency of the test was shifted with eccentricity ranging from 1 cpd at the fovea to 0.3–0.4 cpd at 25 deg. Our plotted peak achromatic cone contrast sensitivities of around 100 in Fig. 1 and 70 in Fig. 2 are slightly below the optimal contrast sensitivities that have been typically reported in the literature (e.g. Campbell & Robson, 1968). This is probably due to the minor influence of several factors, including monocular rather than binocular viewing of our stimuli (a factor 1.41), and the low number (3) of spatial cycles displayed, which was constrained for the reasons described above. In addition, the relatively low mean luminance level (55 cd m^{-2}) produced by RGB compared to black and white display monitors may limit peak contrast sensitivity. Overall, however, our control experiments on binocular viewing and cycle number suggest that modification of these stimulus parameters would not have a significant influence on the differential sensitivities of the three mechanisms or our comparison of their relative losses.

The differential distribution of red–green and blue–yellow cone opponency in human vision that we report lends strong behavioral support the idea that these systems have distinct neurophysiological origins. The recent anatomical and physiological results in primates (see Introduction) indicate that blue–yellow cone opponency has a separate pathway originating in specialized midget bipolar cells and the small-field bistratified ganglion cells of the retina. There is also evidence suggesting that this pathway remains distinct, passing through the koniocellular layers of the LGN and to the blobs of V1. By contrast, it is thought that red–green cone opponency originates in the midget P cells of the retina that predominate in the central visual field. As yet there is no physiological data on the anatomical distribution of the specialized S cone bipolar or ganglion cells across the visual field. At face value, the psychophysical data suggest that these may be quite uniformly distributed. Furthermore, there is evidence that the substantial overrepresentation of central vision begins in the dLGN and is strongest for P cells (Azzopardi et al., 1999), and this might be the mechanism that boosts red–green opponency over blue–yellow in central vision.

In the paper, we have also highlighted differential statistical limitations on red–green and blue–yellow cone opponency. If cone opponency simply arose from binomial variations of cone types in

the excitatory and inhibitory regions of a receptive field, blue–yellow cone opponency would decline across the visual field much more steeply than red–green. This is in stark contrast to the psychophysical results showing that blue–yellow sensitivity is well maintained. Thus, on statistical grounds we can argue that cone-selective connections are an essential requirement for human blue–yellow cone opponency.

On the other hand, the loss of red–green opponency with eccentricity found in human vision is approximately what would be expected statistically from the binomial variations in unselective cone projections, and so cone-selective projections can only be accepted or rejected on direct empirical grounds. How does the empirical evidence for cone selectivity in primate retina weigh up? Prior to the ganglion cell stage in the primate retina there is no evidence for selective connections for L and M cones (Boycott et al., 1987; Calkins & Sterling, 1996; Boycott & Wassle, 1999). In addition, recordings using *in vitro* preparations in macaque have shown large retinal peripheral midget ganglion cells with mixed L and M cone inputs to receptive-field center and surround (Dacey, 1999). On the other hand, other single-cell recordings in macaque retina have indicated the presence of cone-selective P ganglion cells in the periphery (Reid & Shapley, 1992; Lee et al., 1998; Martin et al., 2001). In particular, Reid and Shapley (1992) and Martin et al. (2001) have recorded from large red–green sensitive neurons in the retina, which would not be expected to arise in any number without the benefit of cone selectivity. One possible way to resolve this controversy is by suggesting that there are mixtures of P ganglion cells with and without spectral antagonism (Calkins & Sterling, 1999), or that there are retinal neurons other than midget P cells available to support red–green color *via* cone-selective connections (Calkins & Sterling, 1996).

Another possibility is that the loss red–green contrast sensitivity across the visual field originates has postretinal origins, involving a decline in the relative numbers of red–green cone opponent compared to achromatic units across eccentricity. There is evidence for an enhanced representation of LGN P cells over M cells in the central compared to peripheral visual field originating at the level of the LGN in macaque (Azzopardi et al., 1999). There are reasons to suggest, however, that this does not account for the loss in red–green over achromatic sensitivity that we report here. Our stimuli (achromatic and chromatic) were presented at low temporal frequencies and mid–low spatial frequencies. Primate lesion experiments show these conditions favor stimulus detection mediated by P cells of the LGN, but not M cells (Merigan, 1991). If these findings can be accurately applied to human vision, we predict that our achromatic and chromatic thresholds are both based on P-cell responses, and a declining ratio of P to M cells across eccentricity will not account for the results.

A further possibility is that peripheral red–green cone opponency is restricted at a cortical level. The binomial calculations given earlier have been used to describe cone projections to cone-opponent neurons, but could also be applied to the projection of cone-opponent P cells into cortical neurons. They would thus also predict a loss of red–green sensitivity with eccentricity as cortical units enlarged. There are a number of reasons, however, for rejecting this possibility. Firstly, it predicts that color sensitivity would be limited to small cortical neurons (pooling no more than 4–5 presynaptic units into the receptive-field center (see Fig. 4)). This is not supported by physiological results, which indicate relatively low peak spatial frequencies and large receptive-field sizes for chromatic units in the cortex, even in the fovea (e.g. Thorrel et al., 1984). Furthermore, it would predict a uniform distribution of color-sensitive units within the cortical structure, whereas there is some evidence that color sensitivity predominates in the cortical "blobs" (Ts'o & Gilbert, 1988). Lastly, a cortical explanation for the loss in red–green sensitivity would have to account for why a red–green cone-opponent signal that is available in peripheral retina should be selectively discarded at the cortical stage.

Overall, this paper reveals a differential distribution of red–green and blue–yellow opponency across the visual field in human vision. This provides behavioral evidence for distinct pathways for the two cone-opponent systems in human vision, as supported by recent primate neurophysiological and anatomical results.

Acknowledgments

We thank Drs. Marty Banks and David Vaney for helpful discussions of the study. The work was supported by CIHR grant (#MOP-10819) to K.T. Mullen. A University of Queensland travel award to K.T. Mullen is also acknowledged.

References

Anderson S.A., Mullen, K.T. & Hess, R.F. (1991). Human peripheral spatial resolution for achromatic and chromatic stimuli: Limits imposed by optical and retinal factors. *Journal of Physiology* **442**, 47–64.

Azzopardi, P., Jones, K.E. & Cowey, A. (1999). Uneven mapping of magnocellular and parvocellular projections from the lateral geniculate nucleus to the striate cortex in the macaque monkey. *Vision Research* **39**, 2179–2189.

Baird, J.W. (1905). *The Color Sensitivity of the Peripheral Retina*. Published by The Carnegie Institute of Washington, pp. 1–80.

Boycott, B.B., Hopkins, J.M. & Sperling, H.G. (1987). Cone connections of the horizontal cells of the rhesus monkey's retina. *Proceedings of the Royal Society B* (London), **229**, 345–379.

Boycott, B.B. & Wassle, H. (1999). Parallel processing in the mammalian retina. *Investigative Ophthalmology and Visual Science* **40**, 1313–1327.

Calkins, D.J. & Sterling, P. (1996). Absence of spectrally specific lateral inputs to midget ganglion cells in primate retina. *Nature* **381**, 613–615.

Calkins, D.J. & Sterling, P. (1999). Evidence that circuits in spatial and color vision segregate at the first retinal synapse. *Neuron* **24**, 313–321.

Calkins, D.J., Tsukamoto, Y. & Sterling, P. (1998). Microcircuitry and mosaic of a blue–yellow ganglion cell in the primate retina. *Journal of Neuroscience* **18**, 3373–3385.

Campbell, F.W. & Robson, J.G. (1968). Application of Fourier analysis to the visibility of gratings. *Journal of Physiology* **197**, 551–566.

Cole, G.R., Hine, T. & McIlhagga, W.H. (1993). Detection mechanisms in L-, M-, and S-cone contrast space. *Journal of the Optical Society of America A* **10**, 38–51.

Croner, L.J. & Kaplan, E. (1995). Receptive fields of P and M ganglion cells across the primate retina. *Vision Research* **35**, 7–24.

Curcio, C.A., Kimberly, A.A., Sloan, K.R., Lerea, C.L., Hurley, J.B., Klock, I.B. & Milam, A.H. (1991). Distribution and morphology of human cone photoreceptors stained with anti-blue opsin. *Journal of Comparative Neurology* **312**, 610–624.

Dacey, D.M. (1993*a*). Morphology of a small field bistratified ganglion cell type in the macaque and human retina: Is it the blue-ON cell? *Visual Neuroscience* **10**, 1081–1098.

Dacey, D.M. (1993*b*). The mosaic of midget ganglion cells in the human retina. *Journal of Neuroscience* **13**, 5334–5355.

Dacey D.M. & Lee, B.B (1994). The 'blue-on' opponent pathway in primate retina originates from a distinct bistratified ganglion cell type. *Nature* **367**, 731–735.

Dacey, D.M. (1996). Circuitry for color coding in the primate retina. *Proceeding of the National Academy of Sciences of the U.S.A.* **93**, 582–588.

Dacey, D.M. (1999). Primate retina: Cell types, circuits and color opponency. *Progress in Retinal and Eye Research* **18**, 737–763.

Derrington, A.M., Krauskopf, J. & Lennie, P. (1984). Chromatic mechanisms in lateral geniculate nucleus of macaque. *Journal of Physiology* **357**, 241–265.

Goodchild, A.K. & Martin, P.R. (1998). The distribution of calcium binding proteins in the lateral geniculate nucleus and visual cortex of a New World monkey, the marmoset *Callithrix jacchus*. *Visual Neuroscience* **15**, 625–641.

Gordon, J. & Abramov, I. (1977). Color vision in the peripheral retina II. Hue and saturation. *Journal of the Optical Society of America* **67**, 202–207.

Gouras, P. (1991). Precortical physiology of colour vision. In *The Perception of Colour,* ed. Gouras, P., Vol. 6 of *Vision and Visual Dysfunction,* ed. Cronly-Dillon, J., pp. 163–178. London: Macmillan Press.

Granger, E.M. & Heurtley, J.C. (1973). Visual chromaticity-modulation transfer. *Journal of the Optical Society of America* **63**, 1173–1174.

Hendry, S.H.C. & Reid, R.C. (2000). The koniocellular pathway in primate vision. *Annual Reviews of Neuroscience* **23**, 127–153.

Humanski, R.A. & Wilson, H.R. (1992). Spatial frequency mechanisms with short-wavelength-sensitive cone inputs. *Vision Research* **32**, 549–560.

Kelly, D.H. (1983). Spatiotemporal variation of chromatic and achromatic contrast thresholds. *Journal of the Optical Society of America* **73**, 742–750.

Krauskopf, J., Williams, D.R. & Heeley, D.W. (1982). Cardinal directions of color space. *Vision Research* **22**, 1123–1131.

Lee, B.B., Kremers, J. & Yeh, T. (1998). Receptive field of primate retinal ganglion cells studied with a novel technique. *Visual Neuroscience* **15**, 161–175.

Lee, B.B., Valberg, A., Tigwell, S.A. & Tryti, J. (1987). An account of responses of spectrally opponent neurons in macaque lateral geniculate nucleus to successive contrast. *Proceedings of the Royal Society B* (London) **230**, 293–314.

Lennie, P., Krauskopf, J. & Sclar, G. (1990). Chromatic mechanisms in striate cortex of macaque. *Journal of Neuroscience* **10**, 649–669.

Mariani, A.P. (1984). Bipolar cells in monkey retina selective for the cones likely to be blue-sensitive. *Nature* **308**, 184–186.

Martin, P.R., White, A.J., Goodchild, A.K., Wilder, H.D. & Sefton, A.E. (1997). Evidence that blue-on cells are part of the third geniculocortical pathway in primates. *European Journal of Neuroscience* **9**, 1536–1541.

Martin, P.R., Lee, B.B., White, A.J.R., Solomon, S.G. & Ruttiger, L. (2001). Chromatic sensitivity of ganglion cells in the peripheral retina. *Nature* **410**, 933–936.

Merigan, W.H. (1991). P & M pathway specializations in the macaque. In *From Pigments to Perception,* ed. Valberg, A. & Lee, B.B., pp. 117–125. New York: Plenum Press.

Mollon, J.D. (1989). "Tho she kneel'd in that place where thy grew . . ."—the uses and origins of primate colour vision. *Journal of Experimental Biology* **146**, 21–38.

Mollon, J.D. (1993). Mixing genes and mixing colors. *Current Biology* **3**, 82–85.

Mollon, J.D. & Bowmaker, J.K. (1992). The spatial arrangement of cones in the primate fovea. *Nature* **360**, 677–679.

Mullen, K.T. (1985). The contrast sensitivity of human colour vision to red/green and blue/yellow chromatic gratings. *Journal of Physiology* **359**, 381–400.

Mullen, K.T. (1991). Colour vision as a post receptoral specialization of the central visual field. *Vision Research* **31**, 119–130.

Mullen, K.T. & Kingdom, F.A. (1996). Losses in peripheral color sensitivity predicted from 'hit & miss' post-receptoral cone connections. *Vision Research* **36,** 1995–2000.

Mullen, K.T. & Sankeralli, M.J. (1999). Evidence for the stochastic independence of the blue–yellow, red–green and luminance detection mechanisms revealed by subthreshold summation. *Vision Research* **39**, 733–745.

Mullen, K.T., Beaudot, W.H.A. & McIlhagga, W.H. (2000). Contour integration in color vision: A common process for the blue–yellow, red–green and luminance mechanisms? *Vision Research* **40**, 639–655.

Nathans, J. (1987). Molecular biology of visual pigments. *Annual Review of Neuroscience* **10**, 163–194.

Nathans, J. (1999). The evolution and physiology of human color vision: Insights from molecular genetic studies of visual pigments. *Neuron* **24**, 299–312.

Nathans, J., Thomas, D. & Hogness, D.S. (1986). Molecular genetics of human color vision: The genes encoding blue, green and red pigments. *Science* **232**, 193–202.

Pearson, P.M. & Swanson, W. H. (2000). Chromatic contrast sensitivity: The role of absolute threshold and gain constant in differences between the fovea and the periphery. *Journal of the Optical Society of America A* **17**, 232–43.

Rand, G. (1913). The factors that influence the sensitivity of the retina to color: A quantitative study and methods of standardization. *Psychological Monographs* **15**(62), 1–166.

Reid, R.C. & Shapley, R.M. (1992). Spatial structure of cone inputs to receptive fields in primate lateral geniculate nucleus. *Nature* **356**, 716–718.

Rodieck, R.W. & Watanabe, M. (1993). Survey of the morphology of macaque retinal ganglion cells that project to the pretectum, superior colliculus and parvocellular laminae of the lateral geniculate nucleus. *Journal of Comparative Neurology* **338**, 280–303.

Sankeralli, M.J. & Mullen, K.T. (1996). Estimation of the L-, M- and S-cone weights of the post-receptoral detection mechanisms. *Journal of the Optical Society of America A* **13**, 906–915.

Sankeralli, M.J. & Mullen, K.T. (1997). Postreceptoral chromatic detection mechanisms revealed by noise masking in three-dimensional cone contrast space. *Journal of the Optical Society of America A* **14**, 2633–2646.

Shapley, R. & Perry, V.H. (1986). Cat and monkey retinal ganglion cells and their visual functional roles. *Trends in Neuroscience* **9**, 229–235.

Stromeyer, C.F., III, Lee, J. & Eskew, R.T., Jr. (1992). Peripheral chromatic sensitivity for flashes: A post-receptoral red–green asymmetry. *Vision Research* **32**, 1865–1873.

Stromeyer, C.F., III, Chaparro, A., Tolias, A.S. & Kronauer, R.E. (1997). Colour adaptation modifies the long-wave versus middle-wave cone weights and temporal phases in human luminance (but not red–green) mechanism. *Journal of the Physiology* **499**, 227–254.

Thorrel, L.G., De Valois, R.L. & Albrecht, D.G. (1984). Spatial mapping of monkey V1 cells with pure color and luminance stimuli. *Vision Research* **24**, 751–769.

Ts'o, D.Y. & Gilbert, C.D. (1988). The organization of chromatic and spatial interactions in the primate striate cortex. *Journal of Neurophysiology* **8**, 1712–1727.

Valberg, A., Lee, B.B. & Tigwell, D.A. (1986). Neurons with strong inhibitory S-cone inputs in the macaque lateral geniculate nucleus. *Vision Research* **26**, 1061–1064.

van Esch, J.A., Koldenhof, E.E., van Doorn, A.J. & Koenderink, J.J. (1984). Spectral sensitivity and wavelength discrimination of the human peripheral visual field. *Journal of the Optical Society of America A* **1**, 443–450.

Wassle, H., Grunhert, U., Martin, P.R. & Boycott, B.B. (1994). Immunocytochemical characterization and spatial distribution of midget bipolar cells in the macaque monkey retina. *Vision Research* **34**, 561–580.

Appendix 1: Calculations of average cone-opponent purity

A different proportion of cone types in the inhibitory and excitatory regions of a receptive field is required for a neuron to be cone opponent and thus color sensitive. We calculate how the differential distribution of S cones to the center and surround of a model receptive field varies by chance as the size of the cone group increases. We use as our example a center–surround unit with six times as many cones in the surround than the center, and with equal gains for the center and surround. We define a measure of cone-opponent purity as the difference between the cone purities of the center and surround; this value is scaled by a factor of 0.5 so that it ranges from 0 to 1. Thus, the limiting value of 1 represents a unit with a pure S cone center and no S cones in the surround, and 0 represents a unit with the same proportion of S cones in the center and surround. The average cone-opponent purity is calculated by summing the binomial probabilities for all possible combinations and permutations of cones in both the center and surround of a unit:

$$\sum_{j=1}^{N_c}\sum_{k=0}^{N_s} 0.5 * \left|\frac{j}{N_c} - \frac{k}{N_s}\right| * P(j, N_c, p_b) * P(k, N_s, p_b) * \frac{1}{1 - P(0, N_c, P_c)},$$

where N_c is the number of cones in receptive-field center, N_s is the number of cones in receptive-field surround, j is the number of S cones in each

permutation of center, k is the number of S cones in each permutation of surround, $P(j, N_c, p_b)$ is the binomial probability of the cone permutation in the center, and $P(k, N_s, p_b)$ is the binomial probability of the cone permutation in the surround. An S cone unit was defined as one having at least one S cone in the center, hence the lowest j value is 1. We take the probability of the occurrence of an S cone to be 0.07, taken from data on S cone densities in the human retina (Curcio et al., 1991). Curcio et al. (1991) show that human S cone density varies very little between 1 and 25 deg, thus the same S cone probability can be used for all eccentricities. The reduction in S cone density at the fovea is negligible in comparison to the size of our stimuli, and so was ignored.

Calculations for L,M average cone-opponent purity follow similar principles, as outlined in Mullen and Kingdom (1996). Cone purity ranges from 1 (cones all of one type in center, and all of the other type in the surround) to 0 (the same proportion of cones types in center and surround). Average cone-opponent purity sums the binomial probabilities for all possible combinations and permutations of cones in both the center and surround.